eprints@whiterose.ac.uk
https://eprints.whiterose.ac.uk/

Accepted Manuscript

A design algorithm to model fibre paths for manufacturing of structurally optimised composite laminates

G. Gonzalez Lozano, A. Tiwari, C. Turner

A design algorithm to model fibre paths for manufacturing of structurally optimised composite laminates

G. Gonzalez Lozano[a,b*], A. Tiwari[c], C. Turner[a]

[a]Manufacturing and Materials department, School of Aerospace, Transport and Manufacturing (SATM), Cranfield University, Cranfield, Bedfordshire, MK43 0AL, UK
[b]Airbus Group, Innovations, Building 20A1, Golf Course Lane, Filton, Bristol, BS34 7QW, UK
[c]Automatic Control and Systems Engineering department, Amy Johnson Building, The University of Sheffield, Portobello Street, Sheffield, S1 3JD, UK

Abstract

Fibre steering is involved in the development of non-conventional variable stiffness laminates (VSL) with curvilinear paths as well as in the lay-up of conventional laminates with complex shapes. Manufacturability is generally overlooked in design and, as a result, industrial applications do not take advantage of the potential of composite materials. This work develops a design for manufacturing (DFM) tool for the introduction in design of the manufacturing requirements and limitations derived from the fibre placement technology. This tool enables the automatic generation of continuous fibre paths for manufacturing. Results from its application to a plate with a central hole and an aircraft structure – a windshield front fairing – are presented, showing good correlation of resulting manufacturable paths to initial fibre trajectories. The effect of manufacturing constraints is assessed to elucidate the extent to which the structurally optimal design can be reached while conforming to existing manufacturing specifications.

*Corresponding author: Gustavo Gonzalez Lozano, Airbus Group Innovations, Building 20A1, Golf Course Lane, Filton, Bristol, BS34 7QW, UK. Email: g.gonzalezlozano@cranfield.ac.uk Phone: +44(0)755 3737075
Ashutosh Tiwari, Automatic Control and Systems Engineering department, Amy Johnson Building, The University of Sheffield, Portobello Street, Sheffield, S1 3JD, UK. Email: a.tiwari@sheffield.ac.uk Phone: +44 (0)114 2225624
Christopher Turner, Manufacturing department, SATM, Cranfield University, Building 50, Cranfield, Bedfordshire, MK43 0AL, UK. Email: c.j.turner@cranfield.ac.uk Phone: +44 (0) 1234 755264

1 Introduction

Fibre-reinforced composites are traditionally designed by stacking plies built with a discrete set of constant fibre orientation angles: 0°, ±45° and 90° [1]. These designs do not take full advantage of the potential of composite materials [1–3]. Performance improvements can be driven by the lay-up of curvilinear fibres [4,5], which benefits from a better stress distribution and an expanded design space [6,7]. Automated Fibre Placement (AFP) offers the capability of steering individual fibre tows over the surface of a laminate [1,5,8–10]. Due to the variation of stiffness properties associated with the continuous change in fibre orientation of a layer, these structures were termed as variable stiffness laminates (VSL) [11].

Design and manufacturing of composite structures are interdependent [12]. AFP presents a set of limitations that will affect the manufacturability and quality of designed variable stiffness laminates, such as minimum steering radius (smallest radius of the fibres that can be laid without significant defects, like local fibre buckling or ply wrinkling), minimum cut length (shortest length a tow can be laid in a controlled manner), and gaps and overlaps (defects introduced when a course, set of tows laid up in one machine pass, is not laid parallel to an adjacent one). For instance, tow kinking and wrinkling is noticed in the cylinders manufactured by Blom et al. [13] and Wu et al. [14]. Gaps and overlaps are observed in the cylindrical shells manufactured by Wu et al. [14] and the flat

plates manufactured by Tatting and Gürdal [15]. Recently, a new manufacturing technology called continuous tow shearing (CTS) has been developed, avoiding gaps and overlaps at the expense of thickness variation [16,17].

This type of non-conventional laminates shows an increasing interest from the specialised literature. An extensive review on design optimisation methods can be found in Ghiasi et al. [18] and Sabido et al. [19]. Design approaches include aligning the fibres with the principal stress trajectories and load paths [4,20–24] and using lamination parameters to find the optimal stiffness distribution [6,25–40], which is followed by a retrieval of fibre orientations step [6,31,32]. These methods result in an optimal fibre angle distribution, where continuity of the distribution is not guaranteed and manufacturing constraints are difficult to impose. Discontinuities between neighbouring elements are noticed in the optimal fibre orientations in the work of [6,41,42]. The manufacturing of such designs with curvilinear fibres is not possible [42], and post-processing would be required [43]. For instance, introducing constraints to ensure continuity of fibre orientations could alleviate this issue [28,42,44,45].

In addition, to overcome this issue, many authors have employed a functional parametrisation to represent the fibre paths. This approach typically consists of optimising a reference path, and then, a ply is created by replicating this path, either by shifting the reference path in a specified direction (usually x- or y- axis) or by placing adjacent courses parallel to one another. The former leads to the occurrence of gaps and overlaps between adjacent courses, which may affect the performance of the laminate [46]; while the latter will likely result in kinks as the radius of the tows decreases to remain parallel to the reference path.

Linearly varying fibre angles, introduced in [47], has been widely used in the research [5,9,15,46,48–55]. To overcome the reduced design space of a linear fibre path representation, non-linear variations of fibre angles have also been proposed, for example by means of Lagrangian polynomials [56–58], Lobatto-Legendre polynomials [59,60], Bezier curves [17,61,62], splines [63,64], B-splines surfaces [41], NURBS (Non-Uniform Rational B-Splines) [65], and Lagrangian interpolation functions applied to a manufacturing mesh [66,67]. This method reduces the number of design variables an ease the consideration of manufacturing constraints while modelling continuous paths. However, the design space is limited due to the pre-specified set of possibilities [68]. A streamline analogy, also known as a fluid flow analogy, has been employed to compute continuous fibre paths from discrete fibre angles [4,21,23,31,59,69,70].

Other manufacturing features are considered in design, such as minimum curvature radius [12,32,66–68,71–75] and minimum cut length [13]. For laminate analysis, studies have been conducted on capturing the influence of as-manufactured geometry and features such as gaps, overlaps, tow-drops and variable thickness for the analysis of VSL, by means of 3D FE models [48,76–83], analytical methods [84] and experimental tests [13,81,85–87]. A review focused on analysis methods for buckling, failure and vibration was published by Ribeiro et al. [88] and on design for manufacturing by [89].

However, structural optimisation has been the subject of a larger body of research works, where manufacturability is usually neglected. As a result, few examples exist of practical applications of curvilinear fibre laminates. Besides the design of variable stiffness laminates, fibre steering becomes necessary in

high-complexity structures. Frequently, fibre paths cannot follow the designed

constant fibre orientation in a layer due to the part geometry (e.g. double

curvature), which is dealt manually on a case-by-case basis. Hence, generic

capabilities for the design of fibre-steered laminates and analysis of

manufacturing features are required [89].

A design for manufacturing (DFM) software tool is described in this work that

enables the automatic modelling of fibre paths considering manufacturing

constraints of fibre placement technologies. It provides a novel approach to

consider manufacturability of laminates requiring fibre steering. Also, each fibre

path is modelled explicitly and controlled independently, providing higher

flexibility than existing methods. Thus, it contributes to improve the applicability

of advanced laminate designs with curvilinear fibres in industry. Algorithms to

generate continuous paths from discrete angles and to adapt fibre paths to

manufacturing specifications are presented in section 2.1 and 2.2, respectively.

The procedures to analyse manufacturing features, such as curvature radius

and gaps and overlaps are explained in section 3. This tool is applied to a flat

plate with a hole designed with curvilinear fibres and to an aircraft component –

a windshield front fairing – with conventional fibre in section 4. The paper is

concluded in section 5.

2 Tool to design variable stiffness laminates for manufacturing

A software tool for manufacturing analysis and optimisation of fibre steering

named FIPAM (Fibre Paths for Manufacturing) has been developed. It provides

a post-processing of the design configurations from structural optimisation prior to manufacturing. This tool enables the automatic generation of fibre paths (i.e., machine trajectories), imposing manufacturing requirements. It is integrated in CATIA V5, where each path is modelled individually considering constraints to ensure manufacturability.

A two-step approach is proposed that takes as input a discrete fibre angle distribution resulting from structural optimisation, which is initially imported in the CAD environment where the algorithms for Design for Manufacturing are implemented. The method for structural optimisation of variable stiffness laminates was developed by Peeters et al. [68,74,90,91] and comprises an optimisation of the stiffness distribution using lamination parameters [12] and a posterior fibre angle retrieval and optimisation [68,74,90,91]. Structural approximations of the Finite Element (FE) response are used to reduce the required number of FE analyses [92]. The problem is solved using successive approximations, and convergence is guaranteed by introducing a damping function to achieve conservative approximations [93].

In the first step, the input fibre angles, representative of fibre trajectories for a ply, are translated into continuous reference paths using interpolation algorithms (algorithm 1 in section 2.1). Subsequently, manufacturable fibre paths are generated approaching previously defined references, presented in algorithm 2 in section 2.2. An extension to the above algorithm to enable tow-dropping within a ply is described in section 2.3. Constraints for gaps and overlaps, minimum turning radius, course width and curve smoothness are implemented in the process in order to ensure the suitability of resulting fibre

paths to fibre placement technologies and compliance with specific manufacturing requirements. The objective is to minimise the angle deviation from the optimal fibre angle distribution. Methods need to be implemented to analyse whether a laminate design comply with the constraints. For this purpose, an algorithm to compute the gaps and overlaps of the fibre path design of a ply has been developed (algorithm 3 in section 3.1) and a method to calculate the steering radius of curvature of a path is presented in section 3.2. The complete approach is summarised in Figure 1.

A case study of a flat plate with a central hole optimised for stiffness is used in subsequent sections to describe the algorithms. Continuity constraints were imposed to the structural optimisation procedure. The loading condition was shear force (1N) at the top and bottom edges. The boundary conditions were: all sides were restricted to move in z-direction, the top and bottom edges were simply supported and have to stay straight, and the top left node is also constrained in the first (x) and second (y) directions.

2.1 Modelling of continuous fibre paths

The objective of this step is to generate continuous paths following the optimal discrete fibre orientations. The procedure starts by creating a linear segment from an input starting point. The direction of the segment is obtained by interpolation of the fibre angle at the point from the optimal fibre angle distribution. A benchmark of different interpolation methods (e.g. nearest neighbour, akima) motivated the selection of the Kriging method for its better estimate of the intermediate values and computation time. Ordinary Kriging was

implemented using the library of functions XonGrid Interpolation, with the power variogram defined as [94]:

$$\gamma(h_{ij}) = h_{ij}^{\beta}; \ \ with \ 1 \le \beta \le 1.99 \tag{1}$$

Where h denotes the spatial distance between two random variables (data points, $\mathbf{x}_i$ and $\mathbf{x}_j$), expressed by the equation: $h_{ij} = (\mathbf{x}_i, \mathbf{x}_j) = |\mathbf{x}_i - \mathbf{x}_j|$.

The length of the segment (i.e. fineness of the discretisation) is a constant value given as input. The endpoint of the segment is the starting point for the consecutive segment, where a new value for the fibre angle is determined using the Kriging interpolant. This process is repeated iteratively until the segments reach the boundary of the part or ply. From the resulting polylines, splines are modelled and smoothed using CATIA commands (*Spline* and *Curve Smooth*) to comply with the minimum turning radius constraint. The details of the smoothing operation are included in Figure 2 and the analysis of curvature is further explained in section 3.2.

The accuracy of the curves (deviation from optimal angles) depends on the fineness of the discretisation (i.e. the length of the segments). Assuming the orientation of a segment to be always equal to the interpolated orientation at the starting point of this section introduces some inaccuracy to the generated curve. Alternatively, setting its orientation equal to the interpolated orientation of other point within the segment would also yield some deviation from optimal, as this issue is inherent to the discretisation approach.

However, this can be minimised by setting a sufficiently small segment length. Figure 3 shows an analysis of the effect of the segment length (normalised by the curve length for comparison) on both computation time and accuracy of the fibre path using two arbitrary starting points (Figure 3a) to generate a fibre path. Generally, a segment length of approximately 2% of the approximate total curve provides a good compromise between computation time (Figure 3b) and accuracy (Figure 3c). Further refinements of the segment length do not improve the accuracy. In addition, good accuracy is obtained as long as the segment length is lower than the distance between adjacent points from structural optimisation (mesh fineness of the FE used for structural analysis). The remaining deviations are due to: the accuracy of the Kriging interpolation, the fibre angle deviation between the direction of the centreline and the boundaries of the fibre path (a width of four tows has been considered — 25.4 mm), the difference between the optimal angles at the centreline and the path boundaries (only the centrelines of the fibre paths, which are the generated curves, follow the optimal fibre orientations). The impact of these factors depends on the curve features, as observed by the different slopes in the linear trend in Figure 3c. For example, the effect of the fibre angle deviation on parallel lines is accented in curves with higher curvature, which also indicates a higher variance of the optimal orientations between close points.

The width of each course (machine pass) can be specified and the proportion between gap and overlap size (coverage) is controlled (Figure 4). The selection of next starting points is done iteratively based on the specified course width. Firstly, a point is chosen, which is contained in a parallel curve to the previous

path with an offset equal to the course width (the middle point by default). The

proportion of gaps and overlaps between the original reference and the one

created from the new starting point are computed (method further described in

section 3.1). The position of the starting point is tuned until the required

coverage is met (as guideline, less than five loops are enough for most curves).

This procedure is summarised in algorithm 1. The ply design resulting from

following the optimal angles may present large gaps and overlaps affecting the

manufacturability of the laminate. For a single path, the location of the starting

point along its length does not change the result aside from the effect of the

segment length parameter, discussed earlier in this section. The selection of the

initial starting point mainly influences the position of the resulting curves, but the

general trajectories of the optimal discrete orientations are captured consistently

through continuous paths, which are the input for the next step. For example,

designs with different starting points do not produce intersecting curves.

Algorithm 1 Modelling of continuous reference curves from discrete set of fibre orientations

1. Select starting point
2. Create segment following optimal angle at point
3. Interpolate angle at end of segment
4. Create new segment with the interpolated angle and the end of the previous segment as start point
5. If curve is not finished (cover the surface) then go to 3
6. Join the segments to create a polyline or store the points of start/end of segments to fit a curve.
7. Curve fitting. Options: using the reference points as inputs, create cubic Bezier curves through two consecutive reference points, which are joined; create a general Bezier curve of n-degree using the reference points as control points; use the spline command of CATIA (creation of a NUPBS).
8. Curve smoothing: measure minimum radius of curvature (section 3.2) and smooth the curve in case it does not comply with the minimum turning radius.
9. Select next starting point and go to 2. The selection of the starting points is done iteratively, by choosing first a point contained in a parallel curve to the previous reference with an offset equal to the course width. The position of the starting point is tuned to comply with the defined proportion between gaps and overlaps. The method is as follows:
    a. Create continuous reference path (temporary) from chosen starting point.
    b. Analyse gaps and overlaps (algorithm 3 in section 3.1) between current curve

---

and previous one: max/min gap size (G_max and G_min) and max/min overlap size (O_max and O_min).

c. Calculate coverage: $Cov = \frac{(O\_max + O\_min - G\_min)}{G\_max + O\_max} \cdot 100$

d. Check if coverage matches constraints:

If ($|Cov - Cov\_req| > 5$ (tolerance to speed up convergence))

{No compliance. Tune the distance (*d*) to the previous curve by creating a parallel from the current curve at a distance equal to:

$$d = \frac{(Cov\_req - Cov) \cdot (O\_max + G\_max)}{100}$$

Select a point on this new curve (by default the middle point) and go to (a)

Else

Remove temporary curves and Go to 2 (next reference path)

2.2 Modelling of manufacture compliant fibre paths

In a second step, new fibre paths for manufacturing are modelled approaching the previously defined paths. Choosing one curve as starting path, the method consists of defining a feasible region where the next path should be placed to comply with the specifications on course width, maximum gap and maximum overlap. The new path is created within this region trying to approach the trajectory of the closest reference curve from the first step. To create this manufacturable path, several equally distributed points are created on the current fibre path (initially, it is the starting path). The number of points or distance between points is defined at the beginning of the process. Distances are measured from these points to the target reference, normal to the current fibre path. The minimum distance to the target reference is used to calculate how many fibre paths would fit between the source current path and the target according to the course width. If there is no space between the current path and the target reference to create a path, then that reference is ignored and the next nearest reference is used. The feasible region where the fibre path must be contained to comply with the manufacturing constraints is defined by: a parallel curve to the current fibre path with a distance equal to the course width minus

the maximum overlap allowance, and a parallel offset of the course width plus the allowable gap (Figure 5). A set of control points (C_Pt) are generated by offsetting the points created on the current path at a distance normal to the path on the part surface (i.e. on the distance lines between current path and reference). These points must lie inside the feasibility region. For that purpose, the following formulas have been used (2):

$$\begin{cases} C\_Pt(i) = \left((G\_max + O\_max) \cdot \frac{d(i) - d\_min}{d\_max - d\_min}^{\,w} + CW - O\_max \right) \cdot p, \\ \qquad if \ \left(\frac{d\_max - d\_min}{pt_{btw}} \geq (G\_max + O\_max) \right) \end{cases}$$

$$\begin{cases} C\_Pt(i) = \left(\frac{d\_max - d\_min}{pt_{btw}} \cdot \frac{d(i) - d\_min}{d\_max - d\_min}^{\,w} + CW \right) \cdot p, \\ \qquad if \ \left(\frac{d\_max - d\_min}{pt_{btw}} \leq (G\_max) \right) \end{cases} \qquad (2)$$

$$\begin{cases} C\_Pt(i) = \left(\frac{d\_max - d\_min}{pt_{btw}} \cdot \left(\frac{d(i) - d\_min}{d\_max - d\_min}^{\,w} - 1 \right) + CW + G\_max \right) \cdot p, \ Otherwise \end{cases}$$

Where d_max and d_min denote the maximum and minimum distance between the current path and the reference, respectively; $d(i)$ is the distance to the reference of the point(i) on the current path. G_max and O_max are the manufacturing constraints specified for maximum acceptable gaps and overlaps, respectively; pt_{btw} is the number of fibre paths that will be created between the current path and the reference; p is the path number; CW is the course width; and w is a weight factor to decide whether giving more importance to the current path or the reference. The weight value is normally set to 1. Values lower than 1 will result in the fibre path closer to the reference and higher values result in a path closer to the current path. As generally gaps

12

are preferred over overlaps, the formulas prioritise the presence of gaps within the allowable limits; i.e. if possible, it will eliminate overlaps by using the maximum size of gaps permitted. Better fit to the reference curves (and hence, to the optimal fibre angles) is obtained by relaxing the manufacturing constraints. Figure 6 depicts an example of the approaching process to a straight line using different values for the maximum gap allowed.

A spline is fitted through the calculated control points. The path smoothing algorithm described for the first step is also used here to ensure the created spline satisfies the constraint on minimum turning radius. A compromise between minimising angular deviation from the optimal trajectories and reducing gaps, overlaps and tow drop-offs is sought. The process is repeated until completion of the ply, using the new path as current path and the closest curve from the set of reference curves from the first step as new target to approach. The solution procedure is further explained in algorithm 2. Further details on the implementation of gap and overlap analysis and curvature analysis are provided in sections 3.1 and 3.2 respectively.

Algorithm 2: Solution procedure to model fibre paths for manufacturing based on target approach method

1. Input values:
   Set of reference curves
   Manufacturing constants: gap and overlap allowance, number of tows, tow width, gap between tows, minimum turning radius, maximum angle deviation allowed (optional)
   Settings: Accuracy of distance measurements (number of points on curve) and priority (in case not all constraints can be satisfied)
2. Select starting path (= current path)
3. Sort references according to distance to starting path and side with respect to it
4. Define direction of movement (side)
5. Find nearest reference. If Current path intersects reference (and intersections are not enabled) then, go to next reference; else, select that reference as target
6. Measure minimum distance to target reference. Calculate Number of paths in between:

---

pt_{btw}= Round(d_min/CW). If pt_{btw} = 0, go to step 16; else:

7. Calculate origin and end of current path where distances will be calculated. Distances are measured normal to current path
8. Create points on current path equally distributed along the active segment
9. Compute distances to reference measured normal to current path
10. Create control points by offsetting the points on the current path along the distance lines between current path and reference using formulas described in (2) (objective: approach reference and stay in feasibility region)
11. Fit a spline curve through the control points
12. Split and extrapolate curve (fibre path) to cover the surface
13. Check maximum curvature (section 3.2) and smooth new curve if necessary
14. If maximum angle deviation constraint is used, constraints on gaps and overlaps may not be fulfilled. Analyse individual gaps/overlaps (algorithm 3 in section 3.1) between current path and new fibre path and tune position of fibre path if necessary to satisfy the constraint that is prioritised (either maximum gap or maximum overlap)
15. Make Current path = new fibre path, and go to step 6
16. Calculate if ply is completed.

    If reference = last reference on one side then, enable intersections (to ensure coverage of the ply) and go to step 5

    If Side has been completed then: select Starting path = Current path; change orientation (do the other side) and go to step 5

    If all references have been used then, End

2.3 Tow-dropping

Tow-dropping is a technique used in the manufacture of composite laminates, where fibre tows are individually dropped at the boundary of other paths or ply sectors. The algorithms described in previous sections did not consider tow-dropping. This implied that each fibre path would cover the whole ply or surface of the part, starting and ending outside its boundaries, regardless of any overlap with adjacent non-parallel paths. By dropping the tows, the number of overlaps can be reduced (tows are cut when overlapping other courses); thus, the fibre paths can be designed with a better fit to the theoretically optimal fibre angles, as adjacent courses are allowed more variability while still complying with the overlap size constraint. However, it creates resin-rich areas [76], triangular voids, likely to be the onset of early failure [48].

The way the tows are dropped at the interface of other courses or ply contours is defined by the desired coverage. Coverage of 100% will prevent the presence of gaps and 0% will do the same for overlaps. Any coverage different from 100% will result in the appearance of triangular gaps in the ply. Implementing tow-dropping requires modelling fibre paths up to a fibre tow granularity level and considering the minimum cut length (MCL) constraint, as there cannot be tow lengths below the MCL value. The introduction of the MCL constraint may lead to additional overlaps (if a path longer than necessary is laid up) or gaps (if the path is not laid up).

The algorithm estimates the number of tow-drops necessary for the input conditions and the list of fibre paths. The goal would be to minimise the number of drops as they represent discontinuities in the ply lay-up. This process is executed after the modelling of fibre paths for manufacturing (section 2.2). When the contours of two adjacent courses intersect, tows will be dropped. The decision whether to drop the tows from one path or the other can be defined in the input variables (variable named *Dropping Strategy*). The method also estimates the percentage of material waste with respect to the ply area. Material waste is caused by the ends of the tows that lay outside of the ply surface of the component. Every time a course does not end perpendicularly to the ply contour (courses are cut normal to the path trajectory), there will be material beyond the ply. Having a tow shorter than the MCL on the boundary of a ply will lead to additional material waste, as the course needs to be extended outside of the ply.

3 Analysis of manufacturing features of variable stiffness laminates

For the implementation of manufacturing constraints in the algorithms discussed in section 2, tools to analyse these manufacturing features are required. Specifically, methods to compute the gaps and overlaps of a particular fibre path design and to calculate the minimum curvature radius are presented.

3.1 Analysis of gaps and overlaps

Gaps and overlaps are automatically modelled in CATIA, which enables an evaluation of this design constraint and a visual representation in the model. The inputs are the set of fibre paths defining the ply, the course width and the ply shape (boundary of the ply on the part). Gaps and overlaps are calculated between pairs of adjacent paths iteratively. The fibre paths represent the centrelines of the courses. Parallel lines are created to model the edges of the courses with a distance of half the course width from the input path. The intersections between the outer edge of one path and the inner edge of the other are computed and sorted. The regions delimited by two consecutive intersection points and the path edges define either a gap or an overlap. It depends on the side of the outer and inner edges of the pair of paths. Metrics are calculated for these regions: maximum size of the gap or overlap and area of the gap or overlap. The process is repeated until all gaps and overlaps have been estimated. The procedure is summarised in algorithm 3.

Algorithm 3: Solution procedure to compute gaps and overlaps
1. Sort fibre paths so that they are consecutive
2. Select two adjacent paths to start
3. Compute edges (boundaries) of the fibre paths
○ Create parallel path: Distance = CourseWidth/2

- o Extend and split parallel with curvature continuity to cover the surface
4. Compute intersection points of adjacent fibre path boundaries
5. Sort intersection points
6. Identify whether area limited by intersection points and path boundaries represents a gap or an overlap (if there is no intersection, the whole area between the boundaries will be either a gap or an overlap)
7. Perform measures of the gap/overlap regions: area and maximum size.
8. Select next two adjacent fibre paths and return to step 3
9. Calculate total area, maximum and minimum values of gaps and overlaps of the ply and percentage of gaps/overlaps regarding the area of the surface
10. Generate a text file with the results: global gap/overlap values for the ply and individual gap/overlaps for each pair of adjacent fibre paths

3.2 Measure of radius of curvature

The curvature (κ) is mathematically expressed as (3):

$$\kappa(t) = \|\boldsymbol{\alpha}''(t)\| = \|\boldsymbol{T}'(t)\| \qquad (3)$$

κ is the curvature, $\boldsymbol{\alpha}$ is a curve parametrised by its arc length, and $\boldsymbol{T}$ is the derivative of $\boldsymbol{\alpha}$, which is a unit vector tangent to the curve. The radius of curvature is the inverse of the curvature. For curves on surfaces, further measures of curvature can be defined: the geodesic curvature (κ_g), the normal curvature (κ_n), and the geodesic torsion (τ_r). The normal curvature is the curvature of the curve projected onto the plane containing the curve's tangent $\boldsymbol{T}$ and the surface normal $\boldsymbol{n}$; the geodesic torsion measures the rate of change of the surface normal around the curve's tangent; and the geodesic curvature is the curvature of the curve projected onto the surface's tangent plane [95]. The latter measures how far the curve is from being a geodesic (curve with zero geodesic curvature). These magnitudes are related by the Frenet formulas, where the curvature verifies the following relationships (4):

$$\kappa^2(t) = \kappa_n^2(t) + \kappa_g^2(t) ; \quad \boldsymbol{\alpha}''(t) = \kappa_n(t) \cdot \boldsymbol{n}(t) + \kappa_g(t) \cdot (\boldsymbol{n}(t) \times \boldsymbol{T}(t)) \qquad (4)$$

17

For fibre placement, the interest lies in the geodesic curvature. This is the magnitude that defines the steering of the fibres. Thus, it is the value to which the constraint on maximum allowable curvature is applied. The normal curvature will measure the curvature of the surface in the direction of the curve's tangent. This induces a deflection of the fibres in the out-of-plane direction, which does not represent an issue. The placement head is positioned normal to the surface during lay-up, although certain tilt angle between the head and laying surface is possible.

For flat surfaces, it is apparent that, given a null value of the surface's curvature ($\kappa_n = 0$), the curvature at any point on the curve is equal to the geodesic curvature ($\kappa_g = \kappa$). Indeed, the geodesic curvature is just the usual curvature but when the curve is restricted to lie on a surface.

As explicit parametrisations of the curves are not available when modelling curves in CATIA, the concept of curvature has been implemented through its geometrical interpretation. For space curves, the given minimum radius of curvature would be the radius of the osculating circle to the curve, in agreement with equation (3), instead of the geodesic curvature. The geodesic curvature at a point P can be calculated by doing the orthogonal projection of the tangents to the curve of two infinitely close points ($\boldsymbol{\alpha}(t_p)$ and $\boldsymbol{\alpha}(t_p + \Delta t)$ $\Delta t \to 0$) onto the tangent plane to the surface, and measuring the angle between them (see Figure 7). To avoid instability of the measurements, $\Delta t \geq 0.001\ mm$. The minimum curvature is estimated by getting the minimum value of a sufficiently fine partition of the curve.

18

4　Results

4.1　Design of flat square plate with a hole

The variable stiffness design of a plate with a circular cut-out loaded in tension
and optimised for strength has been undertaken. The details of the structural
optimisation are found in Peeters et al. [68]. The laminate is composed of 6
independent plies. The laminate is assumed to be balanced and symmetric,
leading to a total of 24 layers (thickness of 4.6 mm). The manufacturing
constraints and design of the case study is described in Figure 8.

The optimal fibre angle distribution is converted to continuous fibre paths in the
first step. A segment length of 10 mm was used to create the paths. These
reference paths represent the structurally optimal paths, or the closest the
optimal fibre angle distribution can be matched by continuous curves. Then,
paths for manufacturing are modelled obeying the constraints on maximum gap
and overlap. Initially, tow-dropping is not allowed and a constraint to limit the
maximum allowable angle deviation from optimal has not been imposed.
Otherwise, the combination of constraints may not lead to a feasible solution.
Results for the reference paths and paths for manufacturing are depicted in
Table 1 and Figure 9, including the respective analysis of gaps (in green) and
overlaps (in blue). The resulting maximum angle deviation is lower than 22° for
all plies and the average angle deviation is inferior to 8°. Locally, large angle
deviations are observed due to the small gap size allowed.

To further analyse the relationship between maximum angle deviation from
structural optimal and gaps/overlaps, the design of ply 4 has been revised
introducing a constraint on maximum allowable angle deviation of 5°.

Considering that the optimised ply had a maximum angle deviation = 17.66°, larger gaps and overlaps than the manufacturing requirements will appear. Two alternative designs have been modelled: (i) without prioritising between gaps or overlaps; (ii) prioritising the gap constraint. The results are shown in Table 2. For comparison, it includes the results for the reference paths (that correspond to a 0° maximum deviation constraint) and the optimal paths when the constraint is not imposed. It shows the reduction of gaps and overlaps as the maximum allowable angle deviation constraint is relaxed. The gaps and overlaps of each design are modelled in Figure 10. When introducing a constraint of 5° maximum angle deviation, the manufacturing constraints cannot be satisfied.

Lastly, the number of overlaps can be avoided by dropping tows. Figure 11 shows the ply with the modelling of tows. A Minimum Cut Length (MCL) of 80 mm and a tow-dropping coverage of 10% were applied. The first design (no priority between gaps and overlaps) requires a total of 11 tow-drops, while the second one (priority to meet the gap constraint) needs 27 tow-drops. The reference paths would require a total of 22 tow-drops to remove overlaps of up to 12 mm in size while still presenting large gaps. The fibre paths for manufacturing without imposing the maximum allowable angle deviation constraint do not require tow-dropping, as it has been designed without overlaps. The constraint on maximum allowable angle deviation is applied to the centreline of the path. The resulting maximum angle deviation is a couple of degrees higher than the imposed constraint due to the effect of the course width and optimal orientations at points far from the paths' centreline.

4.2 Design of a windshield front fairing

This structure has a double curved shape with reinforcement areas. It is an
aircraft component designed with conventional straight orientations (0°, ±45°
and 90°). Thus, a fibre path design for manufacturing should be provided for 0°,
45° and 90° fibre orientations. Given the symmetry of the structure with respect
to X-axis, the -45° ply design is obtained from the +45° ply by symmetry with
respect to XZ plane. The location of the part in the aircraft is shown in Figure
12.

The manufacturing constraints and case study are summarised in Figure 13.
There is a minimum steering radius of 1000 mm, courses of 8 tows and a gap
allowance of 2.5 mm. A constraint on maximum allowable angle deviation of ±3°
must be satisfied. The objective is to provide a fibre path design complying with
all the manufacturing constraints. If no feasible solution is possible within the
available angle deviation, the compliance with the gap constraint is prioritised.

The reference paths have been modelled with a segment length between
interpolation steps (accuracy) of 10 mm. The number of overlaps of the
reference paths represents the worst-case scenario, when no fibre angle
deviations from the designed ply orientation are allowed. The fibre paths are
modified for overlap minimisation using the allowed angle deviation of ±3°. The
settings for the path modelling for manufacturing algorithm were: *accuracy* =
250 points per path (number of control points, C_Pt, per path) and *weight* = 1
(parameter w in formula (2), section 2.2). The analysis of gaps and overlaps for
the reference paths and the fibre paths for manufacturing are plotted in Figure

21

14. The results are presented in Table 3. The manufacturing optimisation enables a reduction of the overlap area with respect to the reference paths of 26.3%, 57.3%, and 99.9% for 0°, 45° and 90° ply orientations, respectively. Furthermore, the maximum overlap size experiences a decrease of 4.7%, 10.3% and 96.4% from the reference paths following constant angle orientations. The ±3° angle deviation freedom is proved insufficient to eliminate overlaps for 0° and 45° plies, which for the optimal paths reach sizes over 20 mm, although the density of overlaps is significantly reduced. This lower area of overlaps will lead to fewer tow-drops if dropping tows is acceptable. For the 90° ply, the reference paths do not yield large overlaps and they can be completely eliminated with angle deviations below 3°. The gap area increases as a result of the objective to minimise overlaps, although in a much inferior proportion than the overlap area reduction, and, in every case, respecting the maximum allowable gap size constraint. The maximum size of overlaps does not show a substantial reduction. That can be explained by the accumulation of the ±3° angle deviation for subsequent paths. The ±3° are used to remove overlaps initially from the first paths, and then, as the new paths for manufacturing are already deviated that amount, no further deviation is allowed and the flexibility to modify the paths is constrained. From a global view of the ply, the density of overlaps and general size of overlaps between paths have improved considerably. However, high sizes can still appear locally between some individual adjacent paths.

5   Conclusions

The potential of fibre steering is limited by current manufacturing constraints of fibre placement technologies and design specifications. A novel approach to automatically model fibre paths based on structurally optimised fibre angle distributions and considering manufacturing requirements is proposed. This approach enables to design variable stiffness laminates with curvilinear paths as well as conventional complex structures that require fibre steering. Algorithms are described that create continuous paths following a discrete fibre angle distribution and modify these fibre paths subject to constraints on gaps and overlaps, minimum steering radius, course width and minimum cut length. Each fibre path is modelled and controlled independently. The outcome is a set of manufacturable fibre paths.

The algorithms have been successfully applied to design a series of structures with fibre steering for manufacturing by AFP. Complying with the specified manufacturing constraints and industrial specifications comes at the expense of fitness to the structurally optimal fibre angle distribution with the negative impact on the mechanical response. However, results show good correlation to the optimal fibre angle distribution. The design and manufacturing requirements are inputs that can be defined in the algorithms. With regard to the maximum allowable gap, maximum allowable overlap and maximum allowable angle deviation, only two out of three may be usually successfully imposed. The tool proposed in this research enables prioritising between these constraints. The algorithms are designed to minimise gaps, overlaps and angle deviation.

Therefore, solutions obtained will minimise the discrepancy with respect to those constraints not met for a particular case study.

Overall, this tool improves the manufacturability of fibre-steered laminates by controlling gaps, overlaps and path curvature. Results are promising and indicate that high improvements in the manufacturability of variable stiffness laminates are possible through dedicated DFM methods and algorithms. As the manufacturing variables are captured in the design process, variance between designed and manufactured parts can be reduced. Future advances in the AFP technology and composite materials will help to foster the use of laminates with curvilinear fibres and extend their applicability, with special emphasis on the relaxation of the maximum steering constraint.

Acknowledgements

References

[1]   Sebaey TA, González EV, Lopes CS, Blanco N, Costa J. Damage resistance and damage tolerance of dispersed CFRP laminates: Design and optimization. Compos Struct 2013;95:569–76. doi:10.1016/j.compstruct.2012.07.005.

[2]   Temmen H, Degenhardt R, Raible T. Tailored fibre placement optimisation tool. ICAS, 25th Int. Congr. Aeronaut. Sci., vol. 4, Hamburg, Germany, 3-8 September 2006: Edinburgh: Optimage Ltd; 2006, p. 2462–71.

[3]   Walker M, Smith RE. A technique for the multiobjective optimisation of laminated composite structures using genetic algorithms and finite element analysis. Compos Struct 2003;62:123–8. doi:10.1016/S0263-8223(03)00098-9.

[4]   Tosh MW, Kelly DW. Fibre steering for a composite C-beam. Compos Struct 2001;53:133–41. doi:10.1016/S0263-8223(00)00184-7.

[5] Lopes CS, Gürdal Z, Camanho P. Variable-stiffness composite panels: Buckling and first-ply failure improvements over straight-fibre laminates. Comput Struct 2008;86:897–907. doi:10.1016/j.compstruc.2007.04.016.

[6] Setoodeh S. Optimal design of variable-stiffness fiber-reinforced composites using Cellular Automata. Delft University of Technology, 2005.

[7] Lukaszewicz DH-J a., Ward C, Potter KD. The engineering aspects of automated prepreg layup: History, present and future. Compos Part B Eng 2012;43:997–1009. doi:10.1016/j.compositesb.2011.12.003.

[8] Lopes CS, Camanho PP, Gürdal Z, Tatting BF. Progressive failure analysis of tow-placed, variable-stiffness composite panels. Int J Solids Struct 2007;44:8493–516. doi:10.1016/j.ijsolstr.2007.06.029.

[9] Lopes CS, Gürdal Z, Camanho PP. Tailoring for strength of composite steered-fibre panels with cutouts. Compos Part A Appl Sci Manuf 2010;41:1760–7. doi:10.1016/j.compositesa.2010.08.011.

[10] Evans DO. Fiber placement. In: Miracle DB, Donaldson SL, editors. ASM Handb., Ohio: ASM International; 2001, p. 1135–40.

[11] Gürdal Z, Olmedo R. Composite laminates with spatially varying fiber orientations: Variable Stiffness panel concept. AIAA J 1993;31:751–8.

[12] Ijsselmuiden ST. Optimal design of variable stiffness composite structures using lamination parameters. Delft University of Technology, 2011.

[13] Blom AW, Stickler PB, Gürdal Z. Design and manufacture of a variable-stiffness cylindrical shell. Proc. SAMPE Eur. 30th Int. Conf., SAMPE Europe; 2009, p. 1–8.

[14] Wu KC, Tatting BF, Smith BH, Stevens RS, Occhipinti GP, Swift JB, et al. Design and manufacturing of tow-steered composite shells using fiber placement. 50th AIAA/ASME/ASCE/AHS/ASC Struct. Struct. Dyn. Mater. Conf., Palm Springs, California, USA, 4 - 7 May 2009: AIAA; 2009, p. 1–18. doi:10.2514/6.2009-2700.

[15] Tatting BF, Gürdal Z. Design and manufacture of elastically tailored tow placed plates. Hampton, VA: Langley Research Center: 2002.

[16] Kim BC, Hazra K, Weaver PM, Potter KD. Limitations of fibre placement techniques for variable angle tow composites and their process-induced defects. 18th Int. Conf. Compos. Mater., Jeju, South Korea: 2011, p. 1–6.

[17] Kim BC, Potter K, Weaver PM. Continuous tow shearing for manufacturing variable angle tow composites. Compos Part A Appl Sci Manuf 2012;43:1347–56. doi:10.1016/j.compositesa.2012.02.024.

[18] Ghiasi H, Fayazbakhsh K, Pasini D, Lessard L. Optimum stacking sequence design of composite materials Part II: Variable stiffness design. Compos Struct 2010;93:1–13. doi:10.1016/j.compstruct.2010.06.001.

[19] Sabido A, Bahamonde L, Harik R, van Tooren MJL. Maturity assessment of the laminate variable stiffness design process. Compos Struct 2017;160:804–12. doi:10.1016/j.compstruct.2016.10.081.

[20] Hyer MW, Charette RF. Use of curvilinear fiber format in composite structure design. AIAA J 1991;29:1011–5.

[21] Tosh MW, Kelly DW. On the design , manufacture and testing of trajectorial fibre steering for carbon fibre composite laminates. Compos Part A Appl Sci Manuf

2000;31:1047–60. doi:10.1016/S1359-835X(00)00063-4.

[22]   Crosky A, Kelly D, Li R, Legrand X, Huong N, Ujjin R. Improvement of bearing strength of laminated composites. Compos Struct 2006;76:260–71. doi:10.1016/j.compstruct.2006.06.036.

[23]   Mills A, Patel Z, Frost M, Dell'Anno G. Resin transfer moulding of highly loaded carbon fibre composite aircraft spars using novel fabrics and tow placement techniques. SAMPE J 2007;43:67–72.

[24]   Rolfes R, Tessmer J, Degenhardt R, Temmen H, Bürmann P, Juhasz J. New design tools for lightweight aerospace structures. In: B.H.V. Topping CAMS, editor. Proc. Seventh Int. Conf. Comput. Struct. Technol., Lisbon, Portugal: Saxe-Coburg Publications; 2004, p. 1–30.

[25]   Setoodeh S, Abdalla MM, Gürdal Z. Design of variable-stiffness laminates using lamination parameters. Compos Part B Eng 2006;37:301–9. doi:10.1016/j.compositesb.2005.12.001.

[26]   White SC, Weaver PM. Bend-free shells under uniform pressure with variable-angle tow derived anisotropy. Compos Struct 2012;94:3207–14. doi:10.1016/j.compstruct.2012.05.009.

[27]   Khani A, IJsselmuiden ST, Abdalla MM, Gürdal Z. Design of variable stiffness panels for maximum strength using lamination parameters. Compos Part B Eng 2011;42:546–52. doi:10.1016/j.compositesb.2010.11.005.

[28]   Abdalla MM, Setoodeh S, Gürdal Z. Design of variable stiffness composite panels for maximum fundamental frequency using lamination parameters. Compos Struct 2007;81:283–91. doi:10.1016/j.compstruct.2006.08.018.

[29]   Raju G, Wu Z, Weaver P. On Further Developments of the Feasible Region of Lamination Parameters for Composite Laminates. 55th AIAA/ASME/ASCE/AHS/ASC Struct Struct Dyn Mater Conf 2014:1–13. doi:10.2514/6.2014-1374.

[30]   Ijsselmuiden ST, Abdalla MM, Gürdal Z. Optimization of variable-stiffness panels for maximum buckling load using lamination parameters. AIAA J 2010;48:134–43. doi:10.2514/1.42490.

[31]   van Campen JMJF, Kassapoglou C, Gürdal Z. Design of fiber-steered variable-stiffness laminates based on a given lamination parameters distribution. 52nd AIAA/ASME/ASCE/AHS/ASC Struct. Struct. Dyn. Mater. Conf., 4 - 7 April 2011, Denver, Colorado, USA: AIAA; 2011, p. AIAA 2011-1894. doi:10.2514/6.2011-1894.

[32]   van Campen JMJF, Kassapoglou C, Gürdal Z. Generating realistic laminate fiber angle distributions for optimal variable stiffness laminates. Compos Part B Eng 2012;43:354–60. doi:10.1016/j.compositesb.2011.10.014.

[33]   Ijsselmuiden ST, Abdalla MM, Gürdal Z. Thermomechanical design optimization of variable stiffness composite panels for buckling. J Therm Stress 2010;33:977–92. doi:10.1080/01495739.2010.510701.

[34]   Ijsselmuiden ST, Abdalla MM, Gürdal Z. Thickness tailoring of variable stiffness panels for maximum buckling load. 17th Int. Conf. Compos. Mater., Edinburgh, UK: 2009, p. 1–10.

[35]   Ijsselmuiden ST, Abdalla MM, Gürdal Z. Maximising buckling loads of variable stiffness shells using lamination parameters. 50th AIAA/ASME/ASCE/AHS/ASC Struct. Struct. Dyn. Mater. Conf., Reston, Virigina: American Institute of Aeronautics and Astronautics; 2009, p. 2556. doi:10.2514/6.2009-2556.

[36]   Raju G, White S, Wu Z, Weaver PM. Optimal Postbuckling Design of Variable Angle Tow Composites using Lamination Parameters. 56rd AIAA/ASME/ASCE/AHS/ASC Struct Struct Dyn Mater Conf 2015:1–21.

[37]   Wu Z, Raju G, White S, Weaver PM. Optimal Design of Postbuckling Behaviour of Laminated Composite Plates using Lamination Parameters. 55th AIAA/ASME/ASCE/AHS/ASC Struct Struct Dyn Mater Conf 2014:1–15. doi:10.2514/6.2014-1376.

[38]   Thuwis G a a, De Breuker R, Abdalla MM, Gürdal Z. Aeroelastic tailoring using lamination parameters : Drag reduction of a Formula One rear wing. Struct Multidiscip Optim 2010;41:637–46. doi:10.1007/s00158-009-0437-6.

[39]   Stanford BK, Jutte C V. Comparison of curvilinear stiffeners and tow steered composites for aeroelastic tailoring of aircraft wings. Comput Struct 2017;183:48–60. doi:10.1016/j.compstruc.2017.01.010.

[40]   Thuwis G a a, Abdalla MM, Gürdal Z. Optimization of a variable-stiffness skin for morphing high-lift devices. Smart Mater Struct 2010;19:124010. doi:10.1088/0964-1726/19/12/124010.

[41]   Montemurro M, Catapano A. On the effective integration of manufacturability constraints within the multi-scale methodology for designing variable angle-tow laminates. Compos Struct 2017;161:145–59. doi:10.1016/j.compstruct.2016.11.018.

[42]   Setoodeh S, Gürdal Z, Watson LT. Design of variable-stiffness composite layers using cellular automata. Comput Methods Appl Mech Eng 2006;195:836–51. doi:10.1016/j.cma.2005.03.005.

[43]   Sørensen R, Kann J. Optimisation of composite structures using lamination parameters in a finite element application. Aalborg University, 2011.

[44]   Setoodeh S, Abdalla MM, IJsselmuiden ST, Gürdal Z. Design of variable-stiffness composite panels for maximum buckling load. Compos Struct 2009;87:109–17. doi:10.1016/j.compstruct.2008.01.008.

[45]   Setoodeh S, Gürdal Z. Design of composite layers with curvilinear fiber paths using cellular automata. 44th AIAA/ASME/ASCE/AHS Struct. Struct. Dyn. Mater. Conf., Virginia, USA: AIAA; 2003.

[46]   Tatting BF. Analysis and design of variable stiffness composite cylinders. Virginia Polytechnic Institute, 1998.

[47]   Olmedo R, Gürdal Z. Buckling response of laminates with spatially varying fiber orientations. 34th AIAA/ASME/ASCE/AHS/ASC Struct. Struct. Dyn. Mater. Conf., La Jolla, CA, USA; ; 19 April 1993 through 22 April 1993: AIAA; 1993, p. Vol. 4, pp. 2261–9.

[48]   Lopes CS. Damage and failure of non-conventional composite laminates. Delft University of Technology, 2009.

[49]   Zamani Z, Haddadpour H, Ghazavi MR. Curvilinear fiber optimization tools for design thin walled beams. Thin-Walled Struct 2011;49:448–54. doi:10.1016/j.tws.2010.08.002.

[50]   Haddadpour H, Zamani Z. Curvilinear fiber optimization tools for aeroelastic design of composite wings. J Fluids Struct 2012;33:180–90. doi:10.1016/j.jfluidstructs.2012.05.008.

[51]   Stanford BK, Jutte C V., Wu CK. Aeroelastic benefits of tow steering for composite plates. Compos Struct 2014;118:416–22. doi:10.1016/j.compstruct.2014.08.007.

[52]   Alhajahmad A, Abdalla MM, Gürdal Z. Optimal design of tow-placed fuselage panels for maximum strength with buckling considerations. AIAA J Aircr 2010;47:775–82. doi:10.2514/1.40357.

[53]   Akhavan H, Ribeiro P. Geometrically non-linear periodic forced vibrations of imperfect laminates with curved fibres by the shooting method. Compos Part B Eng 2017;109:286–96. doi:10.1016/j.compositesb.2016.10.059.

[54]   Samukham S, Raju G, Vyasarayani CP. Parametric instabilities of variable angle tow composite laminate under axial compression. Compos Struct 2017;166:229–38. doi:10.1016/j.compstruct.2017.01.044.

[55]   Haldar A, Reinoso J, Jansen E, Rolfes R. Thermally induced multistable configurations of variable stiffness composite plates: Semi-analytical and finite element investigation. Compos Struct 2017. doi:10.1016/j.compstruct.2017.02.014.

[56]   Wu Z, Weaver PM, Raju G, Kim BC, Chul Kim B. Buckling analysis and optimisation of variable angle tow composite plates. Thin-Walled Struct 2012;60:163–72. doi:10.1016/j.tws.2012.07.008.

[57]   Wu Z, Weaver PM, Raju G. Postbuckling optimisation of variable angle tow composite plates. Compos Struct 2013;103:34–42. doi:10.1016/j.compstruct.2013.03.004.

[58]   Guimaraes TA, Castro SG, Rade DA, Cesnik CE. Panel Flutter Analysis and Optimization of Composite Tow Steered Plates. 58th AIAA/ASCE/AHS/ASC Struct. Struct. Dyn. Mater. Conf., 2017. doi:10.2514/6.2017-1118.

[59]   Alhajahmad A, Abdalla MM, Gürdal Z. Design Tailoring for Pressure Pillowing Using Tow-Placed Steered Fibers. AIAA J Aircr 2008;45:630–40. doi:10.2514/1.32676.

[60]   Demasi L, Santarpia E, Cavallaro R, Biagini G, Vannucci F. Equivalent Single Layer, Zig-Zag and Layer wise theories for Variable-Stiffness composite laminates based on the Generalized Unified Formulation. 58th AIAA/ASCE/AHS/ASC Struct. Struct. Dyn. Mater. Conf., 2017, p. 1–34. doi:10.2514/6.2017-0891.

[61]   Dems K, Wiśniewski J. Optimal design of fibre-reinforced composite disks. J Theor Appl Mech 2009;47:515–35.

[62]   Parnas L, Oral S, Ceyhan Ü. Optimum design of composite structures with curved fiber courses. Compos Sci Technol 2003;63:1071–82. doi:10.1016/S0266-3538(02)00312-3.

[63]   Honda S, Narita Y. Natural frequencies and vibration modes of laminated composite plates reinforced with arbitrary curvilinear fiber shape paths. J Sound Vib 2012;331:180–91. doi:10.1016/j.jsv.2011.08.019.

[64]   Honda S, Narita Y, Sasaki K. Maximizing the Fundamental Frequency of Laminated Composite Plates with Optimally Shaped Curvilinear Fibers. J Syst Des Dyn 2009;3:867–76. doi:10.1299/jsdd.3.867.

[65]   Nagendra S, Kodiyalam S, Davis JE, Parthasarathy VN. Optimization of tow fiber paths for composite design. 36th AIAA/ASME/ASCE/AHS/ASC Struct. Struct. Dyn. Mater. Conf., vol. 2, New Orleans, LA, USA: AIAA; 1995, p. 1031–41.

[66]   van Tooren MJ, Elham A, Harik R. Optimal variable stiffness distribution for a composite plate with a row of holes subjected to tension/shear load cases. 16th AIAA/ISSMO Multidiscip Anal Optim Conf 2015:1–14. doi:10.2514/6.2015-2488.

[67]   Van Tooren MJ, Jahangir I, Elham A. Optimization of variable stiffness composite plates with cut-outs subjected to compression, tension and shear using an adjoint formulation. 57th AIAA/ASCE/AHS/ASC Struct Struct Dyn Mater Conf 2016:1–17.

doi:10.2514/6.2016-1970.

[68] Peeters DMJ, Abdalla MM. Effect of Steering Limit Constraints on the Performance of Variable Stiffness Laminates. 20th Int. Conf. Compos. Mater. ICCM20, Copenhagen, 19 - 24th July: 2015.

[69] Gliesche K, Hübner T, Orawetz H. Application of the tailored fibre placement (TFP) process for a local reinforcement on an "open-hole" tension plate from carbon/epoxy laminates. Compos Sci Technol 2003;63:81–8.

[70] Charan R, Renault T, Ogale AA, Bagchi A. Automated fiber reinforced composite prototypes. Proc. 5th Int. Conf. Rapid Prototyp., Dayton, Ohio: 1994, p. 91–7.

[71] Waldhart C. Analysis of tow-placed, variable-stiffness laminates. Virginia Polytechnic Institute and State University, Blacksburg, Virginia, USA, 1996.

[72] Waldhart C, Gürdal Z, Ribbens C. Analysis of tow placed, parallel fiber, variable stiffness laminates. 37th AIAA/ASME/ASCE/AHS/ASC Struct. Struct. Dyn. Mater. Conf., vol. 4, Salt Lake City, UT, USA; 15 April 1996 through 17 April 1996: AIAA; 1996, p. 2210–20.

[73] Pilaka VKR. Design of realistic variable stiffness laminates - a gradient-based optimizer for retrieving fiber orientation angles with average curvature constraints from lamination parameter distributions. 2010.

[74] Peeters DMJ, Hesse S, Abdalla MM. Stacking sequence optimisation of variable stiffness laminates with manufacturing constraints. Compos Struct 2015;125:596–604. doi:10.1016/j.compstruct.2015.02.044.

[75] Peeters DMJ, Irisarri F-X, Abdalla MM. Optimizing the ply dropping order in variable stiffness , variable thickness laminates using stacking sequence tables. 17th Eur. Conf. Compos. Mater. ECCM17, Munich, Germnay, 26-30th June: 2016.

[76] Fagiano C. Computational modeling of tow-placed composite laminates with fabrication features. Delft University of Technology, 2010.

[77] Fayazbakhsh K, Arian Nik M, Pasini D, Lessard L. Defect layer method to capture effect of gaps and overlaps in variable stiffness laminates made by Automated Fiber Placement. Compos Struct 2013;97:245–51. doi:10.1016/j.compstruct.2012.10.031.

[78] Kärger L, Kling A. As-built FE simulation of advanced fibre placement structures based on manufacturing data. Compos Struct 2013;100:104–12. doi:10.1016/j.compstruct.2012.11.024.

[79] Rhead a. T, Dodwell TJ, Butler R. The effect of tow gaps on compression after impact strength of AFP laminates. 15th Eur. Conf. Compos. Mater., vol. 35, 2012, p. 1–16.

[80] Rhead a. T, Dodwell TJ, Butler R. The effect of tow gaps on compression after impact strength of robotically laminated structures. Comput Mater Contin 2013;35:1–16.

[81] Dang TD, Hallett SR, Kim BC, Le Cahain Y, Butler R, Liu W. Modelling of as manufactured geometry for prediction of impact and compression after impact behaviour of variable angle tow laminates. J Compos Mater 2014;0:1–16. doi:10.1177/0021998312462619.

[82] Blom AW, Lopes CS, Kromwijk PJ, Gürdal Z, Camanho PP. A theoretical model to study the influence of tow-drop areas on the stiffness and strength of variable-stiffness laminates. J Compos Mater 2009;43:403–25. doi:10.1177/0021998308097675.

[83] Falcó O, Mayugo JA, Lopes CS, Gascons N, Turon A, Costa J. Variable-stiffness composite panels: As-manufactured modeling and its influence on the failure behavior.

29

Compos Part B Eng 2014;56:660–9. doi:10.1016/j.compositesb.2013.09.003.

[84]   Lucas D, Van Tooren MJ, Elham A. Stiffness Corrections for Overlaps and Gaps in Steered Composite Panel Optimization. 58th AIAA/ASCE/AHS/ASC Struct. Struct. Dyn. Mater. Conf., 2017, p. 1–16. doi:10.2514/6.2017-0895.

[85]   Croft K, Lessard L, Pasini D, Hojjati M, Chen J, Yousefpour A. Experimental study of the effect of automated fiber placement induced defects on performance of composite laminates. Compos Part A Appl Sci Manuf 2011;42:484–91. doi:10.1016/j.compositesa.2011.01.007.

[86]   Falcó O, Mayugo JA, Lopes CS, Gascons N, Costa J. Variable-stiffness composite panels: Defect tolerance under in-plane tensile loading. Compos Part A Appl Sci Manuf 2014;63:21–31. doi:10.1016/j.compositesa.2014.03.022.

[87]   Falcó O, Lopes CS, Mayugo JA, Gascons N, Renart J. Effect of tow-drop gaps on the damage resistance and tolerance of Variable-Stiffness Panels. Compos Struct 2014;116:94–103. doi:10.1016/j.compstruct.2014.05.005.

[88]   Ribeiro P, Akhavan H, Teter A, Warmiński J. A review on the mechanical behaviour of curvilinear fibre composite laminated panels. J Compos Mater 2014;48:2761–2777. doi:10.1177/0021998313502066.

[89]   Lozano GG, Tiwari A, Turner C, Astwood S. A review on design for manufacture of variable stiffness composite laminates. Proc Inst Mech Eng Part B J Eng Manuf 2016;230. doi:10.1177/0954405415600012.

[90]   Peeters D, Van Baalen D, Abdallah M. Combining topology and lamination parameter optimisation. Struct Multidiscip Optim 2015:105–20. doi:10.1007/s00158-014-1223-7.

[91]   Peeters DMJ, Abdalla M. Optimization of Ply Drop Locations in Variable-Stiffness Composites. AIAA J 2016;54:1760–8. doi:10.2514/1.J054369.

[92]   de Wit A, van Keulen F. Numerical comparison of multi-level optimization techniques. 48th AIAA/ASME/ASCE/AHS/ASC Struct. Struct. Dyn. Mater. Conf., Honolulu, Hawaii: American Institute of Aeronautics and Astronautics; 2007. doi:doi:10.2514/6.2007-1895.

[93]   Svanberg K. A class of globally convergent optimization methods based on conservative convex separable approximations. SIAM J Optim 2002;12:555–73.

[94]   Deglo de Besses B. XonGrid Interpolation. Version 4 [Software]. 2014. Available at: http://xongrid.sourceforge.net/.

[95]   Do Carmo MP. Differential Geometry of Curves and Surfaces. Englewood Cliffs, New Jersey, USA: Prentice-Hall Inc.; 1976:511.
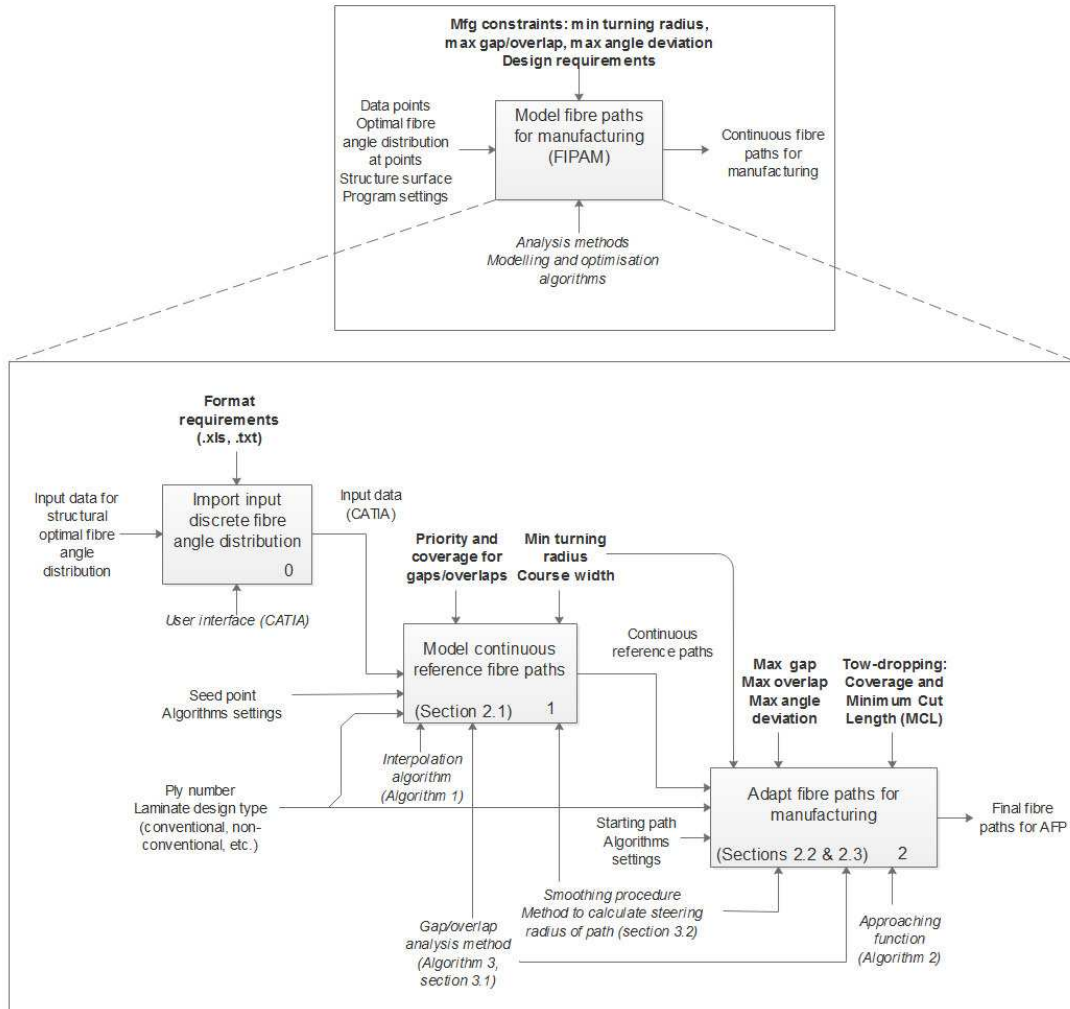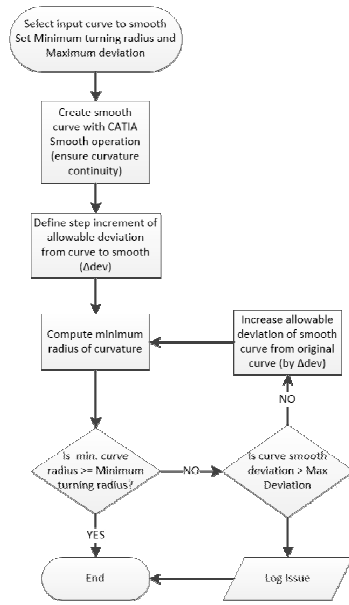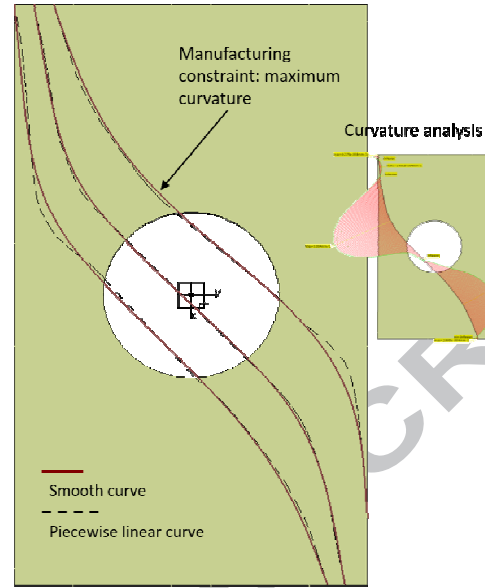
30

Figure 1. Approach for fibre path modelling for manufacturing, including for each step (boxes): input and output variables (left and right side of boxes), conditions and constraints applicable (in bold at top side of boxes), and enablers and algorithms used (in italic at bottom side of boxes).

(a) Flowchart of procedure

(b) Example of smoothing operation on a flat plate

with a hole

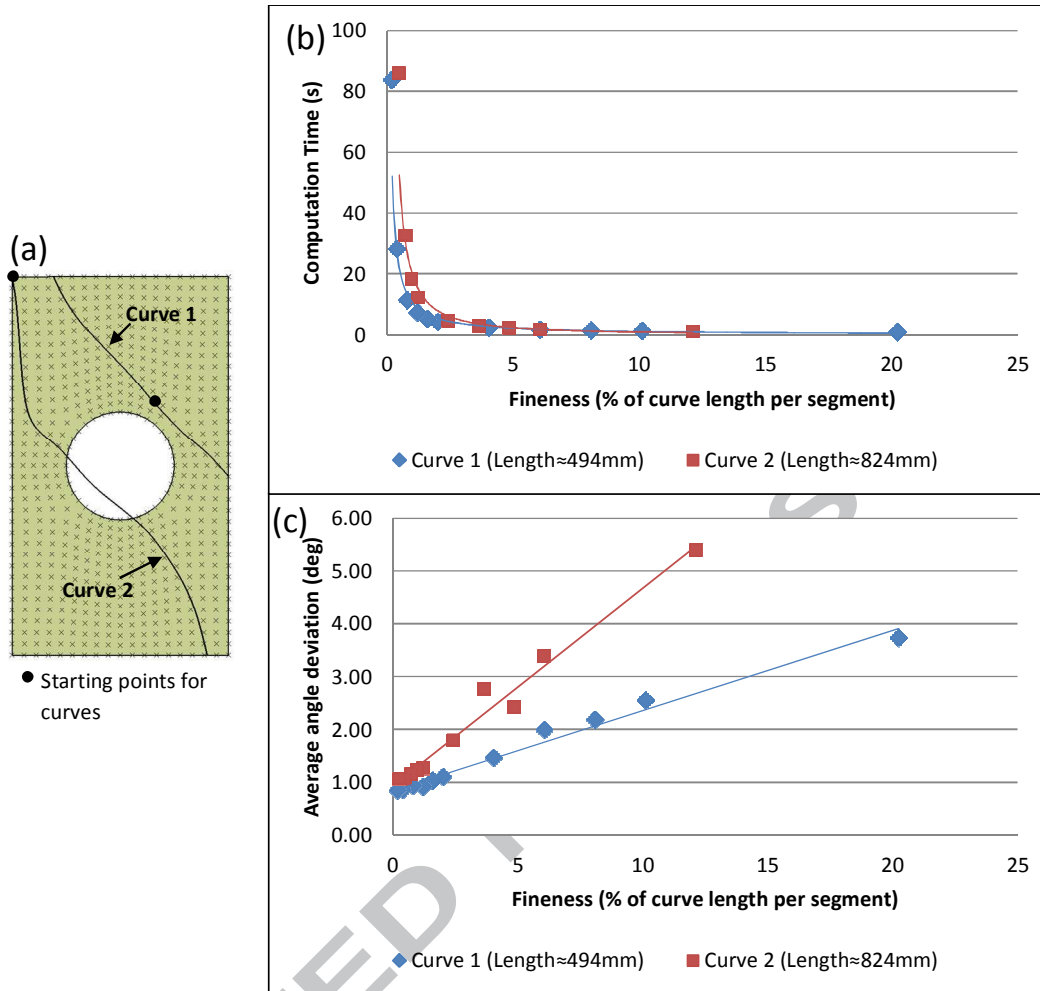**Figure 2.** Curve smoothing approach to comply with minimum turning radius constraint

Figure 3. (a) Case study used and representation of modelled curves; (b) graph of the effect of refinement of interpolation on computation time; (c) graph of the effect of refinement on average angle deviation
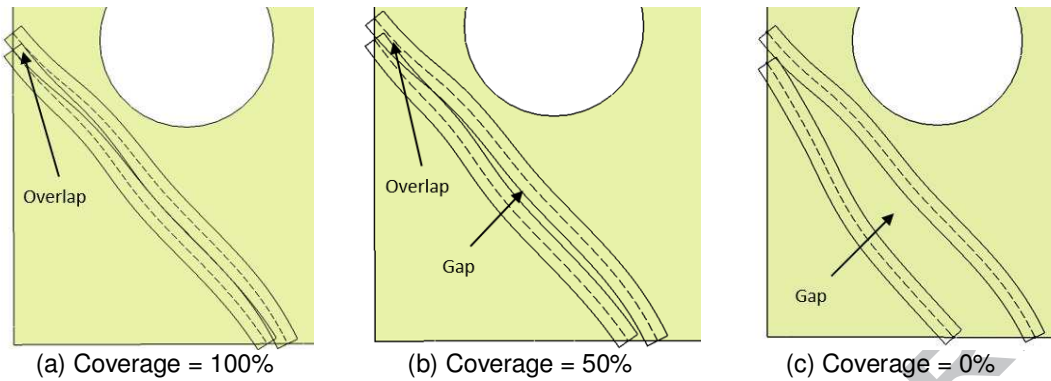
(a) Coverage = 100%   (b) Coverage = 50%   (c) Coverage = 0%

Figure 4. Generation of two reference curves on a plate with a hole with course width = 25.4mm and different input values for gap/overlap proportion (coverage)
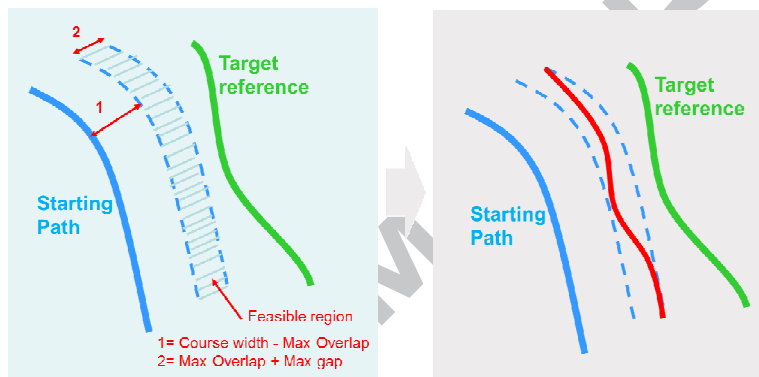

Figure 5. Process rationale to create fibre paths for manufacturing approaching reference curves
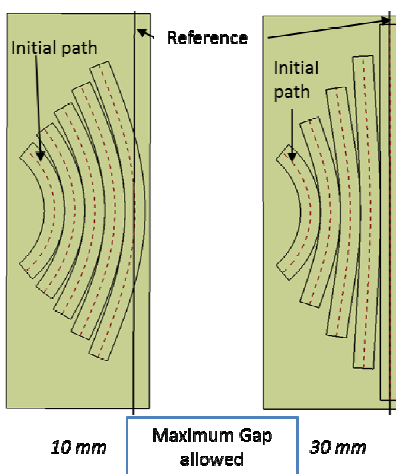

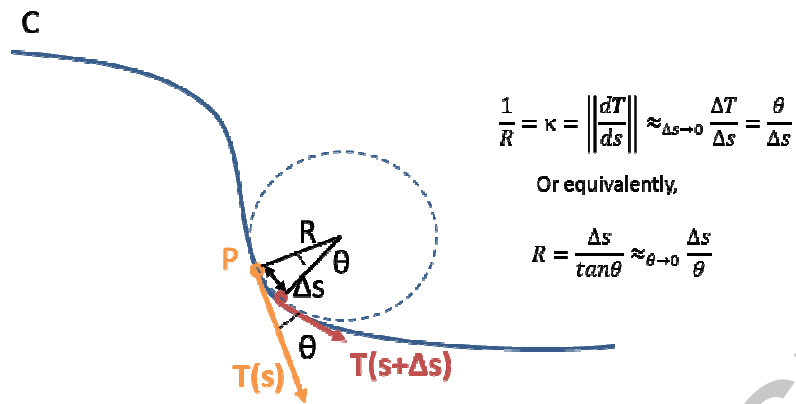**Figure 6.** Fibre paths to approach a straight line with different maximum allowable gaps and no overlaps

$$\frac{1}{R} = \kappa = \left\|\frac{dT}{ds}\right\| \approx_{\Delta s \to 0} \frac{\Delta T}{\Delta s} = \frac{\theta}{\Delta s}$$

Or equivalently,

$$R = \frac{\Delta s}{tan\theta} \approx_{\theta \to 0} \frac{\Delta s}{\theta}$$

Figure 7. Geometrical interpretation of curvature of a curve at point P

FLAT PLATE WITH HOLE

Structural: Strength optimisation

Manufacturing: Minimisation of average and maximum angle deviation

Constraints:
• No overlaps.
• No tow drops.
• Course width = 25.4 mm (4 tows)
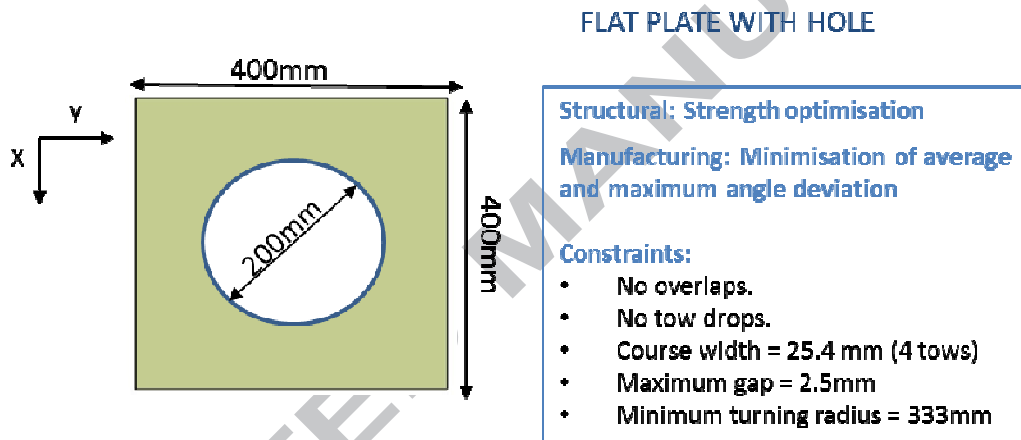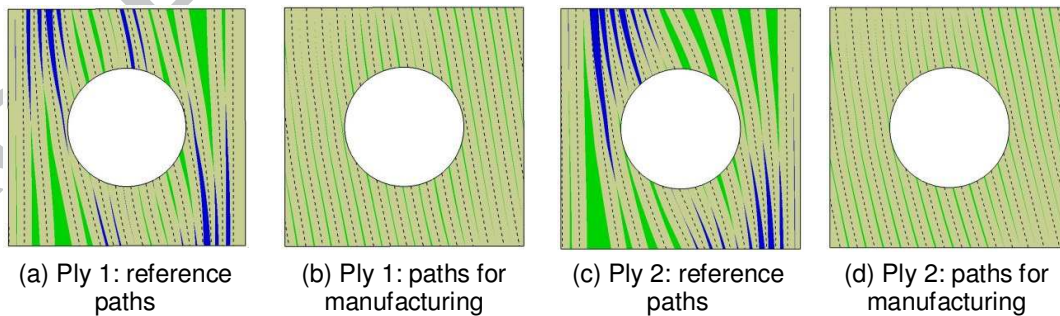• Maximum gap = 2.5mm
• Minimum turning radius = 333mm

Figure 8. Definition of case study for flat square plate with a hole: dimensions, design and manufacturing constraints

(a) Ply 1: reference paths

(b) Ply 1: paths for manufacturing

(c) Ply 2: reference paths

(d) Ply 2: paths for manufacturing

(e) Ply 3: reference paths

(f) Ply 3: paths for manufacturing

(g) Ply 4: reference paths

(h) Ply 4: paths for manufacturing

(i) Ply 5: reference paths

(j) Ply 5: paths for manufacturing

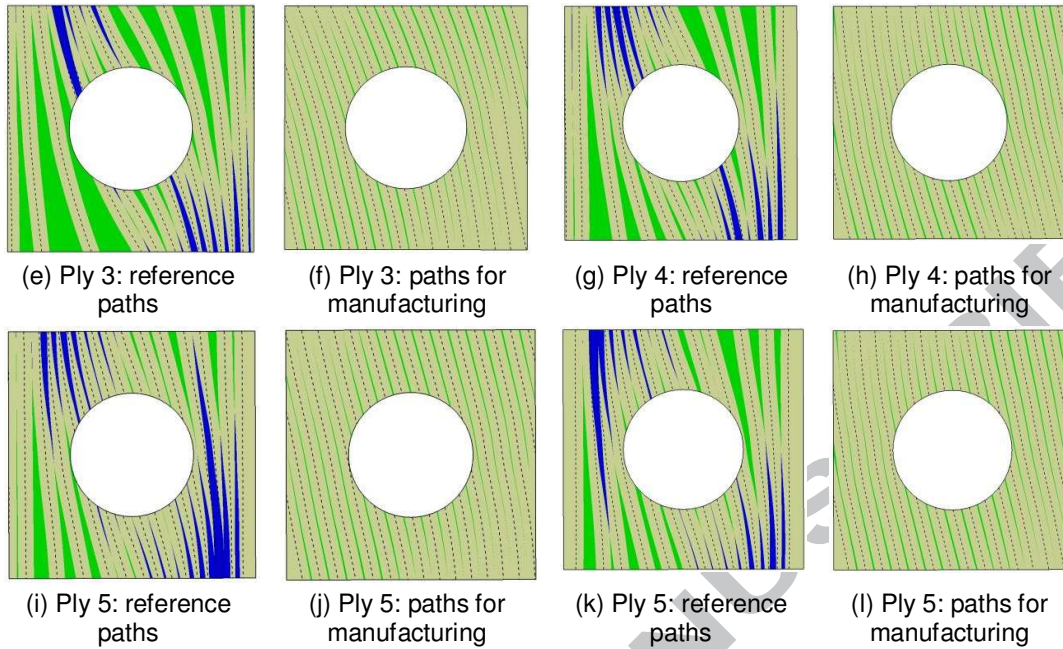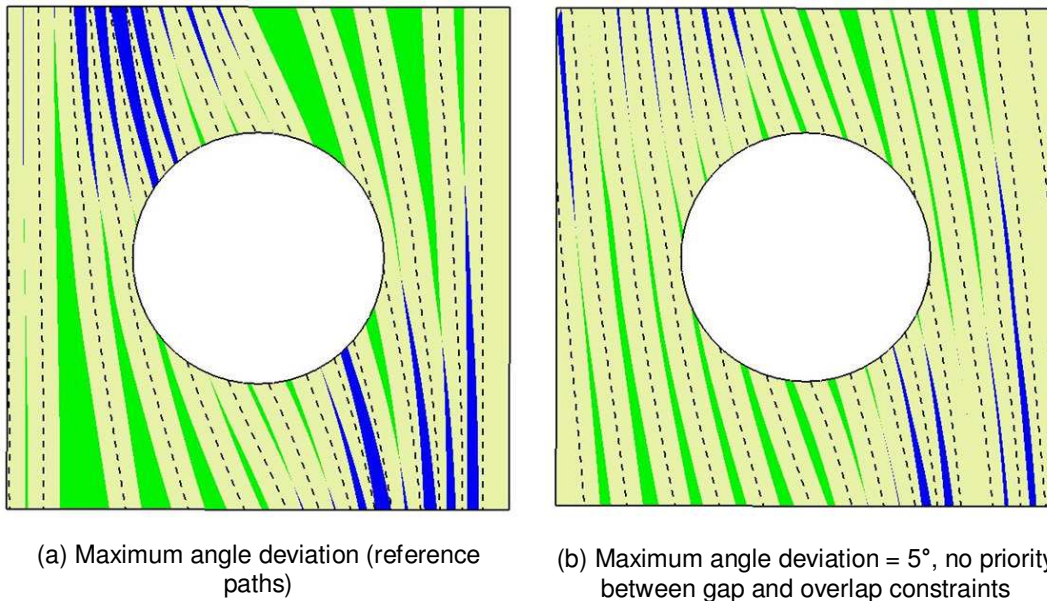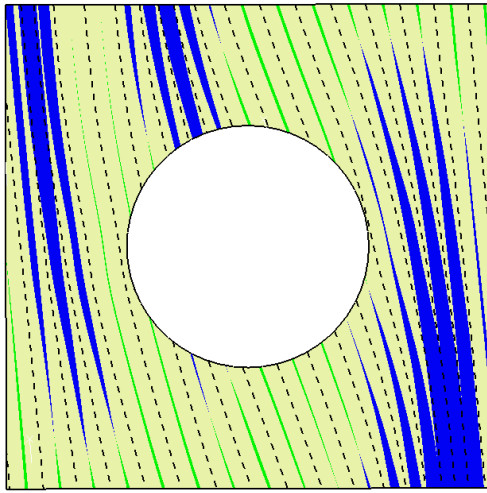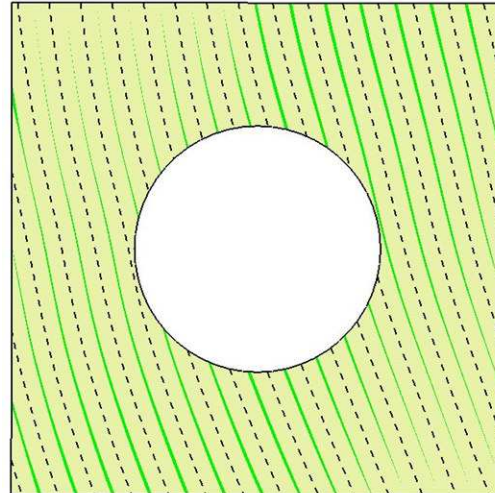(k) Ply 5: reference paths

(l) Ply 5: paths for manufacturing

Figure 9. Flat square plate with a hole: reference paths optimised for structures and paths optimised for manufacturing with gap and overlap analysis for each ply (green: gap and blue: overlap)


(a) Maximum angle deviation (reference paths)

(b) Maximum angle deviation = 5°, no priority between gap and overlap constraints

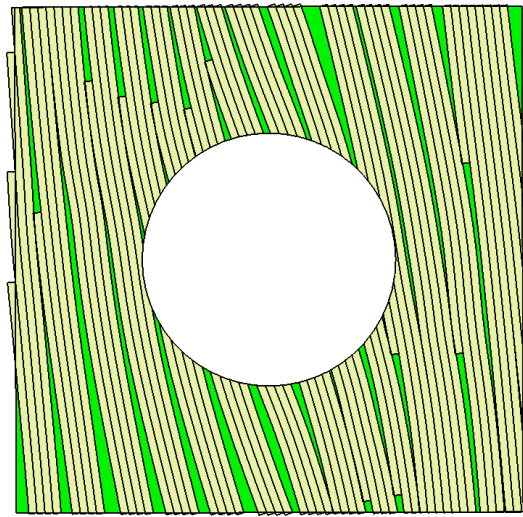(c) Maximum angle deviation = 5°, priority for gap constraint satisfaction

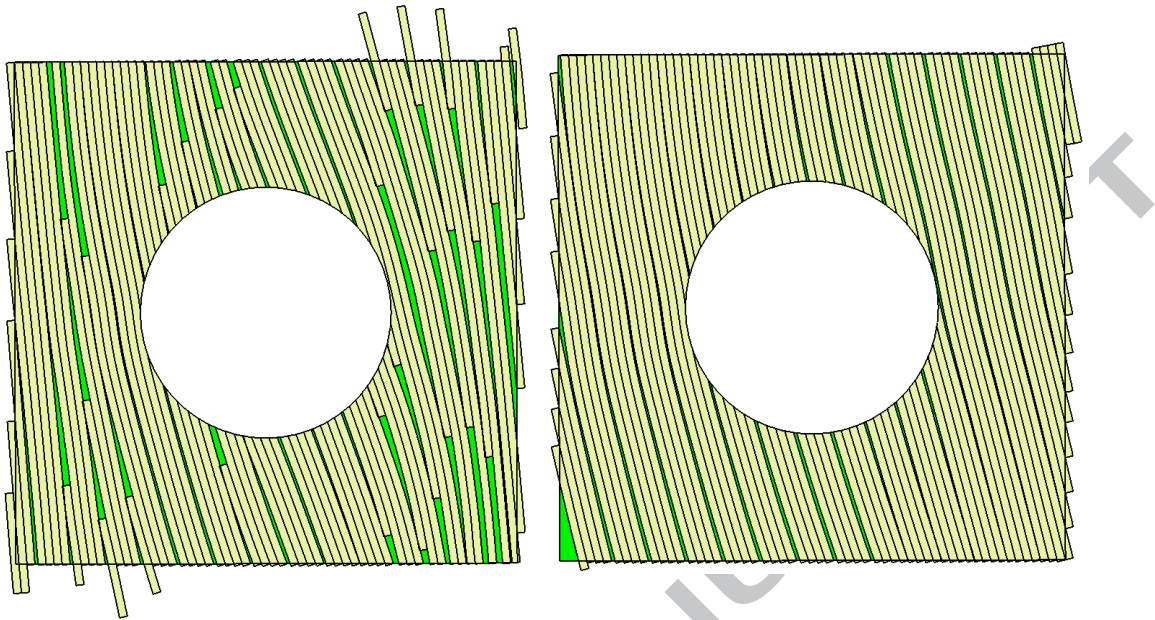(d) Maximum angle deviation = Not applied

Figure 10. Gap and overlap analysis of different design solutions for ply 4 of flat square plate

with a hole (gap: green and overlap: blue)
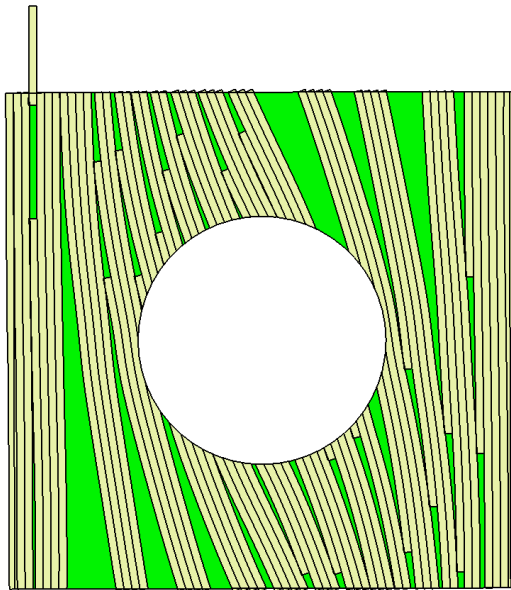
(a) Tow-drops of reference paths. Number = 22 tow-drops

(b) Tow-drops of paths for manufacturing (max angle dev = 5°, and no priority between gap/overlap constraint). Number = 11 tow-drops

(c) Tow-drops of paths for manufacturing (max angle dev = 5°, and priority for compliance with gap constraint). Number = 27 tow-drops

(d) Tow-drops of paths for manufacturing (max angle dev = not applied). Number = 0 tow-drops

Figure 11. Tow modelling of different design solutions with tow-dropping (coverage = 10% overlap; MCL= 80 mm) for ply 4 of flat square plate with a hole
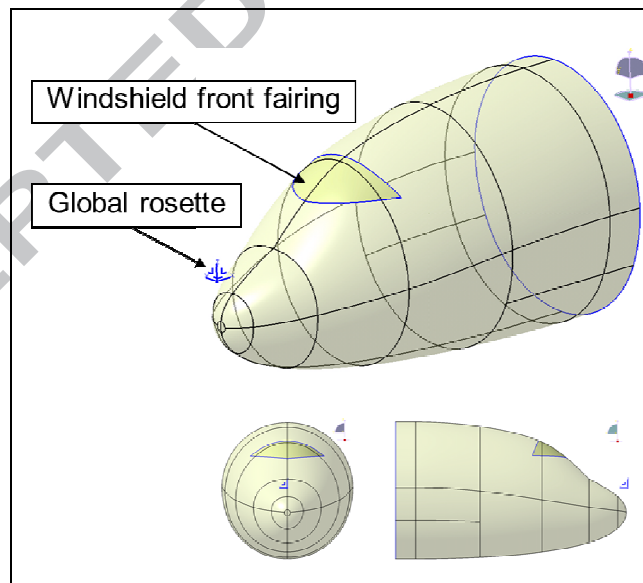

Figure 12. Location of windshield front fairing and axis system on aircraft
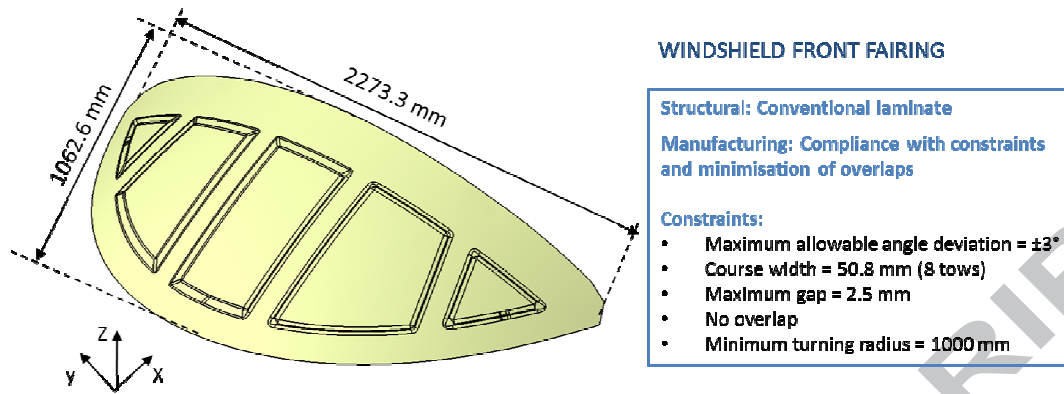
WINDSHIELD FRONT FAIRING

Structural: Conventional laminate

Manufacturing: Compliance with constraints
and minimisation of overlaps

Constraints:
- Maximum allowable angle deviation = ±3°
- Course width = 50.8 mm (8 tows)
- Maximum gap = 2.5 mm
- No overlap
- Minimum turning radius = 1000 mm

Figure 13. Definition of case study for windshield front fairing: dimensions, design and manufacturing constraints

(a) Ply 0°: reference paths

(b) Ply 0°: manufacturing paths

(c) Ply 45°: reference paths

(d) Ply 45°: manufacturing paths

(e) Ply 90°: reference paths
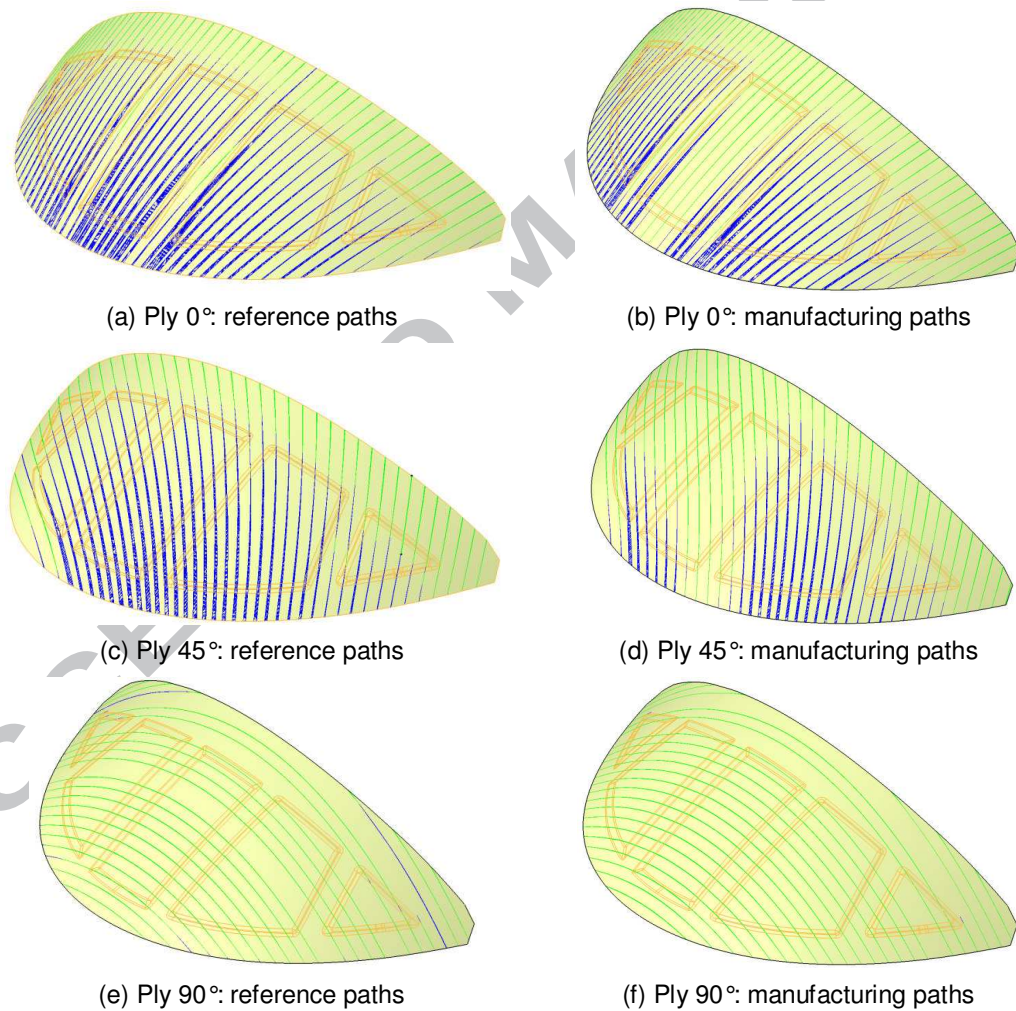
(f) Ply 90°: manufacturing paths

Figure 14. Gap and overlap analysis of reference paths and paths for manufacturing for windshield front fairing

Table 1. Flat square plate with a hole: Analysis of angle deviations of optimal paths for manufacturing

		Ply 1	Ply 2	Ply 3	Ply 4	Ply 5	Ply 6
Angle deviation	**Average (deg)**	3.70	5.843	7.01	6.05	4.61	4.61
	Std deviation (deg)	2.85	4.02	5.13	4.30	3.70	3.54
	Maximum value (deg)	11.03	18.58	21.18	17.66	13.21	13.81

Table 2. Analysis of results of ply 4 of flat square plate with a hole showing angle deviations, gaps and overlaps, and tow-drops that would be needed to remove the overlaps

Case study	Flat square plate with a hole			
Ply	4			
Constraint: maximum allowable angle deviation (deg)	0	5	5	Not applied (>180)
Additional conditions	None	None	Priority for gap constraint	None
Maximum gap size (mm)	39.2	13.7	2.57	2.5
Maximum overlap size (mm)	12.1	7.6	14.94	0.1
Total gap area (%)	15.9	8.8	2.37	4.8
Total overlap area (%)	7.0	2.8	18.91	0.01
Average of angular deviation from optimal (deg)	0.96	3.3	3.92	6.05
Maximum angular deviation from optimal (deg)	4.94	7.1	7.68	17.66
Number of tow-drops to eliminate overlaps	22	11	27	0
Are gap and overlap constraints met?	NO	NO	NO	YES

Table 3. Analysis of results for the design of reference (Ref) and manufacturing (Mfg) fibre paths of windshield front fairing

Case study	Windshield front fairing					
Ply orientation (deg)	0		45		90	
Description	Ref. Paths	Mfg. Paths	Ref. Paths	Mfg. Paths	Ref. Paths	Mfg. Paths
Constraint: maximum allowable angle deviation (deg)	0	3	0	3	0	3
Optimal starting path index	---	1	---	29	---	5
Maximum overlap size (mm)	27.48	26.20	17.33	15.54	2.15	0.077
Maximum gap size (mm)	2.58	2.498	2.59	2.54	2.56	2.56
Total overlap area (%)	10.35	7.63	8.30	3.54	0.060	7.92E-5
Total gap area (%)	0.65	0.91	0.90	1.59	1.79	2.17